Injection Direction Sensitive Spin Lifetime Model in a Strained Thin Silicon Film

Joydeep Ghosh, Dmitry Osintsev, Viktor Sverdlov, and Siegfried Selberherr
Institute for Microelectronics, TU Wien, Gußhausstraße 27–29/E360, A–1040 Wien, Austria
Email: {ghosh|osintsev|sverdlov|selberherr}@iue.tuwien.ac.at

***Abstract*—The electron spin properties are promising for future spin-driven applications. Silicon, the major material of microelectronics, also appears to be a perfect material for spintronic applications. The peculiarities of the subband structure and details of the spin propagation in ultra-thin silicon films in presence of the spin-orbit interaction and strain are investigated. The application of shear strain dramatically reduces the spin relaxation in such films. We investigate in detail, how spin injection in any arbitrary direction modifies the spin relaxation matrix elements, and finally the spin lifetime in the samples. We demonstrate a two-fold enhancement of spin lifetime, when spin is injected in-plane of the sample, compared to that, when injected along the perpendicular-plane direction.**

***Keywords*—Spin relaxation in silicon, spin-orbit interaction, valley-orbit interaction, spin injection, $\mathbf{k}\cdot\mathbf{p}$ model.**

I. Introduction

As devices are scaled down to the nano-scale, fundamental physical limitations will hinder further improvements in device performance in the upcoming years. Employing spin as an additional degree of freedom is promising for boosting the efficiency of future low-power integrated electronic circuits [1]. Silicon, the main material of microelectronics, is primarily composed of nuclei with zero spin and is characterized by weak spin-orbit interaction in the conduction band. Both factors favor achieving a small spin relaxation. A long spin transfer distance of conduction electrons has been shown experimentally [2], hence spin propagation at such distances makes the fabrication of spin-based switching devices quite plausible in the near future. However on the other hand, a large experimentally observed spin relaxation in electrically-gated silicon structures could become an obstacle in realizing spin-driven devices [3]. This drives demands for a deeper understanding of fundamental spin relaxation in silicon.

Shear strain has traditionally been used in industry to boost electron mobility. A several orders of magnitude enhancement of spin lifetime in (001) oriented films subjected to [110] uniaxial tensile stress has been predicted [4]. When the spin injection direction is changed from perpendicular-plane to in-plane, the increment of the surface roughness(SR)-induced spin lifetime has also been elaborated [5]. In addition to SR-mediated spin-flips, the longitudinal(LA)- and transversal(TA)-acoustic phonons, the prominent spin relaxation mechanisms for silicon thin films are also required to be considered. In this work we show, how an arbitrary spin injection direction modifies the subband wave functions, the SR-induced intersubband spin relaxation matrix elements, and finally the total spin lifetime. For an accurate calculation, we also incorporate the valley splitting in un-strained films together with the shear strain induced splitting on equal footing [4].

II. Model

A. $\mathbf{k}\cdot\mathbf{p}$ Hamiltonian with spin

In order to find the corresponding scattering matrix elements, relaxation rates, and the spin lifetime, one has to evaluate the subband structure and the wave functions in the film. For this purpose, the effective two-band $\mathbf{k}\cdot\mathbf{p}$ Hamiltonian including the spin degree of freedom and describing the electron states in the conduction band of the two relevant [001] valleys in the vicinity of the X-point along the k_z-axis in the Brillouin zone must be considered. The $\mathbf{k}\cdot\mathbf{p}$ approach is suitable to describe the electron subband structure and allows to find the wave functions in (001) silicon films in an analytical form, when the confinement potential is approximated by an infinite square well [6]. We also properly take into account the presence of tensile shear strain ε_{xy}, and the spin-orbit interaction [4], [7] in the Hamiltonian:

$$H = \begin{bmatrix} H_1 & H_3 \\ H_3^\dagger & H_2 \end{bmatrix}, \tag{1}$$

where H_1, H_2, and H_3 are written as,

$$H_{j=1,2} = \left[\frac{\hbar^2 k_z^2}{2m_l} + \frac{\hbar^2\left(k_x^2+k_y^2\right)}{2m_t} + \frac{(-1)^j\hbar^2 k_0 k_z}{m_l} + U(z)\right] I \tag{2}$$

$$H_3 = \begin{bmatrix} D\varepsilon_{xy} - \dfrac{\hbar^2 k_x k_y}{M} & (k_y - k_x\mathrm{i})\,\Delta_{SO} \\ (-k_y - k_x\mathrm{i})\,\Delta_{SO} & D\varepsilon_{xy} - \dfrac{\hbar^2 k_x k_y}{M} \end{bmatrix}. \tag{3}$$

Here (k_x, k_y, k_z) represents the projections of the wave vector $\vec{k}$, $k_0 = 0.15\cdot\frac{2\pi}{a}$ is the position of the valley minimum relative to the X-point in unstrained silicon, $U(z)$ is the

Parameter	Value
Silicon lattice constant	$a = 0.5431\,\mathrm{nm}$
Spin-orbit term	$\triangle_{SO} = 1.27\,\mathrm{meVnm}$
Shear deformation potential	$D = 14\,\mathrm{eV}$
Electron rest mass in silicon	m_e
Transversal effective mass	$m_t = 0.19\,m_e$
Longitudinal effective mass	$m_l = 0.91\,m_e$
Valley minimum position from X-point	$k_0 = 0.15\cdot\frac{2\pi}{a}$
Splitting at Γ-point	$\Delta_\Gamma = 5.5\,\mathrm{eV}$
$k_{0\Gamma}$	$k_{0\Gamma} = 0.85\cdot\frac{2\pi}{a}$

TABLE I: Simulation parameter list

978-1-4673-7860-4/15/$31.00 ©2015 IEEE

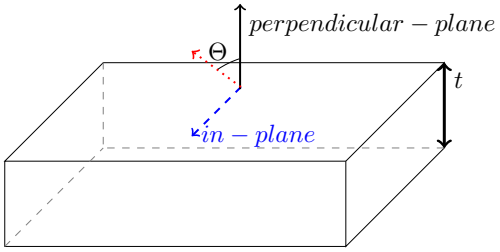

Fig. 1: Sketch showing the spin injection in an arbitrary direction, described by the polar angle Θ.

confinement potential, and the other parameters are defined in Table (I). H_3 describes the coupling of the electron states from the opposite valleys.

In order to solve the Schrödinger equation with the Hamiltonian (1) for the wave functions, the unitary transformation [8] is performed to obtain the new Hamiltonian,

$$H' = \begin{bmatrix} H'_1 & H'_3 \\ H'_3 & H'_2 \end{bmatrix}, \tag{4}$$

with

$$H'_{j=1,2} = \left[\frac{\hbar^2 k_z^2}{2m_l} + \frac{\hbar^2\left(k_x^2+k_y^2\right)}{2m_t} + (-1)^j\delta + U(z)\right] I \tag{5}$$

$$H'_3 = \begin{bmatrix} \frac{\hbar^2 k_0 k_z}{m_l} & 0 \\ 0 & \frac{\hbar^2 k_0 k_z}{m_l} \end{bmatrix}, \tag{6}$$

where

$$\delta = \sqrt{\left(D\varepsilon_{xy} - \frac{\hbar^2 k_x k_y}{M}\right)^2 + \triangle_{SO}^2\cdot(k_x^2+k_y^2) + \Lambda_\Gamma^2}\,. \tag{7}$$

Λ_Γ pertains to the unprimed subband splitting at unstrained silicon (001) films (Table (I)) and can be expressed as [4]:

$$\Lambda_\Gamma = \frac{2\pi^2\Delta_\Gamma}{(k_0\cdot t)^3}\cdot\sin(k_{0\Gamma}t)\,. \tag{8}$$

B. Subband wave functions

The eigenfunctions of (4) for the two lowest unprimed subbands (n=1, 1′) with the up(down)-spin states with the spin quantization axis along the spin-orbit field in (k_x, -k_y) direction are denoted as $\Psi_{n\uparrow}$ ($\Psi_{n\downarrow}$). Considering Θ (Φ) as the polar (azimuthal) angle denoting the spin injection orientation (Figure 1), we must perform linear transformations to obtain the wave functions ($\chi_{n\uparrow}$, $\chi_{n\downarrow}$) with their spin parallel to the injection orientation:

$$\begin{aligned}\chi_{n\uparrow} = &\left(\frac{\cos\frac{\theta}{2}}{\sqrt{2}} + \frac{\sin\frac{\theta}{2}}{\sqrt{2}}\cdot\exp(-i(\phi_1-\phi))\right)\cdot\Psi_{n\uparrow}\\ &+\left(\frac{\cos\frac{\theta}{2}}{\sqrt{2}} - \frac{\sin\frac{\theta}{2}}{\sqrt{2}}\cdot\exp(-i(\phi_1-\phi))\right)\cdot\Psi_{n\downarrow}\,,\end{aligned} \tag{9}$$

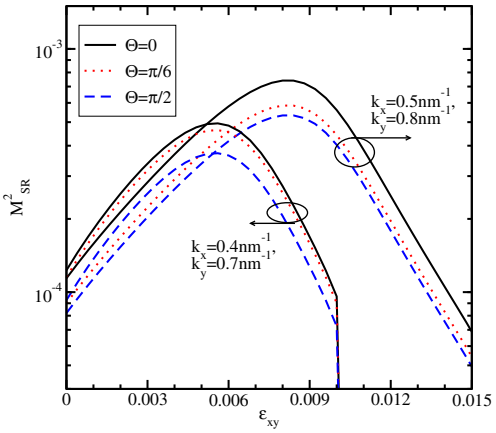

Fig. 2: Intersubband spin relaxation matrix element for surface roughness normalized to intrasubband scattering (M_{SR}) with ε_{xy} and the spin injection angle (Θ). t=1.36nm.

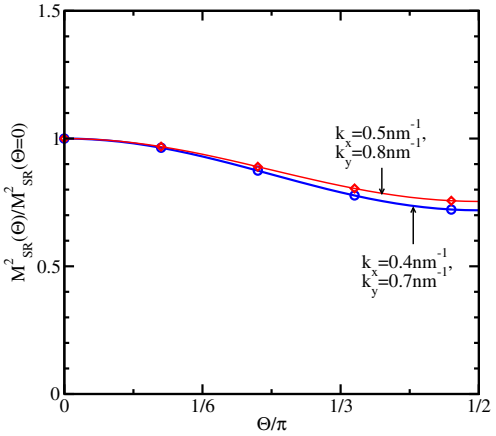

Fig. 3: Variation of M_{SR} with Θ corresponding to Figure 2. Lines: theory, dots: simulation.

$$\begin{aligned}\chi_{n\downarrow} = &\left(\frac{-\sin\frac{\theta}{2}}{\sqrt{2}} + \frac{\cos\frac{\theta}{2}}{\sqrt{2}}\cdot\exp(-i(\phi_1-\phi))\right)\cdot\Psi_{n\uparrow}\\ &+\left(\frac{-\sin\frac{\theta}{2}}{\sqrt{2}} - \frac{\cos\frac{\theta}{2}}{\sqrt{2}}\cdot\exp(-i(\phi_1-\phi))\right)\cdot\Psi_{n\downarrow}\,,\end{aligned} \tag{10}$$

with $\tan\phi_1 = -\frac{k_y}{k_x}$.

III. Results

A. Intersubband Spin Relaxation Matrix Elements

We calculate the normalized intersubband SR-induced spin matrix elements M_{SR}, for arbitrary (k_x, k_y) pairs as [9]:

$$M_{SR} = \left[\frac{\frac{d\chi_{i-\sigma}(z)}{dz}\,\frac{d\chi_{j\sigma}(z)}{dz}}{\left(\frac{d\chi_{i\sigma}(z)}{dz}\,\frac{d\chi_{i\sigma}(z)}{dz}\right)_{\varepsilon_{xy}=0}}\right]_{z=\pm\frac{t}{2}}, \tag{11}$$

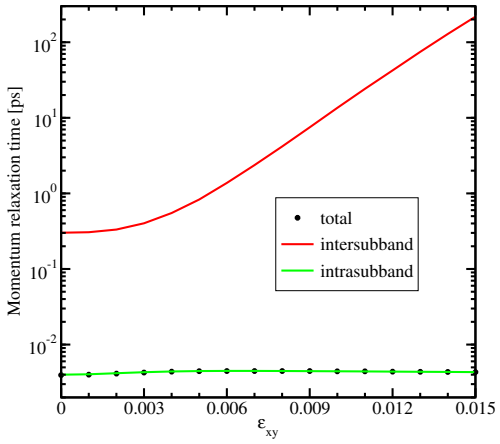

Fig. 4: Variation of momentum relaxation time with ε_{xy}, showing no influence of Θ. t=1.36nm, the electron concentration N_S=10^{12} cm^{-2}.

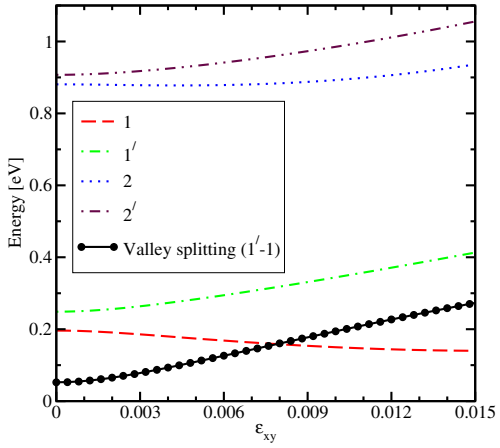

Fig. 5: Degeneracy lifting of the unprimed subbands with ε_{xy}, giving rise to the valley splitting. t=1.36nm.

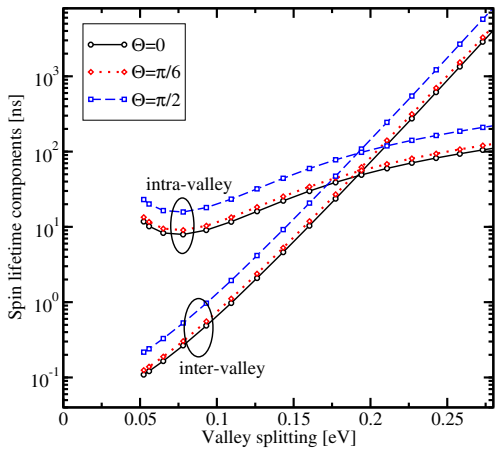

Fig. 6: The dependence of inter- and intrasubband components of τ on the valley splitting, when Θ is used as a parameter. t=1.36nm, N_S=10^{12} cm^{-2}.

with $\sigma = \pm 1$ as the spin projection to the injection axis, and i (j) as the band index. M_{SR} is maximum at the spin hot spots condition (cf. Figure 2),

$$D\varepsilon_{xy} - \frac{\hbar^2 k_x k_y}{M} = 0\,. \tag{12}$$

Here $M^{-1} = m_t^{-1} - m_e^{-1}$. It is noticed that M_{SR} is reduced with increasing Θ. The dependence is well described by,

$$M_{SR} \propto 1 + \left(\frac{k_x}{k_y}\right)^2 \cdot \cos^2\Theta\,. \tag{13}$$

Henceforth it turns out that the spin scattering rate decreases, when spin injection is drawn gradually towards in-plane (Figure 3), for the electron-phonon scattering mediated spin relaxation as well.

B. Momentum and Spin Lifetime

The spin and momentum relaxation times are calculated by the corresponding thermal averaging of the respective subbands' in-plane momentum dependent scattering rates [10], [11]. In Figure 4 we show the momentum relaxation time (τ^M) with its components. It stays unaltered irrespective of the spin injection direction as expected and shows almost a two-fold increase with ε_{xy}. The dominance of the intrasubband relaxation process is in agreement with the selection rule that the elastic processes result in only intrasubband momentum relaxation.

Now we calculate the total spin relaxation time (τ) with its inter- and intrasubband components. The valley-orbit interaction leads to an energy splitting (valley splitting) among the equivalent unprimed subbands in the confined electron system. Figure 5 shows how ε_{xy} inflicts the subband splitting between the unprimed valley pair. This lifting of the degeneracy is the crucial factor for spin lifetime enhancement [4]. We note that the degeneracy between equivalent valleys was a longstanding problem in silicon spintronics. It is also observed that in thin films the lowest unprimed subbands are primarily responsible for determining the spin relaxation rate and spin lifetime. Figure 6 demonstrates the variation of the inter(intra)subband components of τ with the valley splitting taken from Figure 5 and Θ, showing an increase with the valley splitting and also with Θ. In Figure 7 we show how τ increases with the valley splitting and Θ. From Figure 6 and Figure 7 it is confirmed that the major contribution in τ comes from intersubband scattering [12], [13] at low values of the valley splitting (because of the presence of spin hot spots), whereas at higher values the intrasubband component also turns out to be non-negligible. In accordance with Figure 2 we find that, the spin scattering rate (lifetime) decreases (increases) with Θ for all stress points, thus τ attains the maximum for in-plane spin injection. We also note that the ratio of τ as well as its components, computed for different injection directions at the same stress value, does not depend on ε_{xy}.

Now we investigate, how one can express the variation of τ on Θ at any fixed ε_{xy} (or equivalent valley splitting) point. In Figure 8 we highlight the ratio of τ for any arbitrary Θ value compared to that for perpendicular-plane injection at $\varepsilon_{xy} = 0.5\%$. An analytical expression describing this dependence can

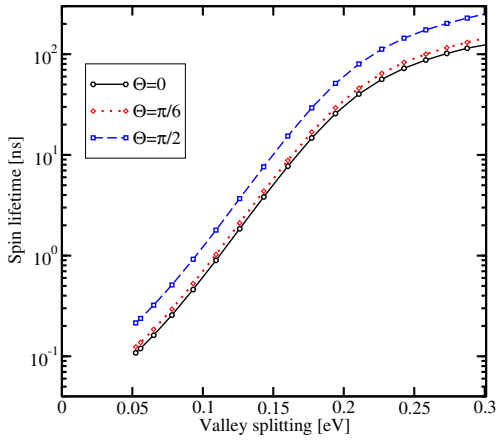

Fig. 7: Variation of τ with the valley splitting from Figure 5, when Θ is used as a parameter.

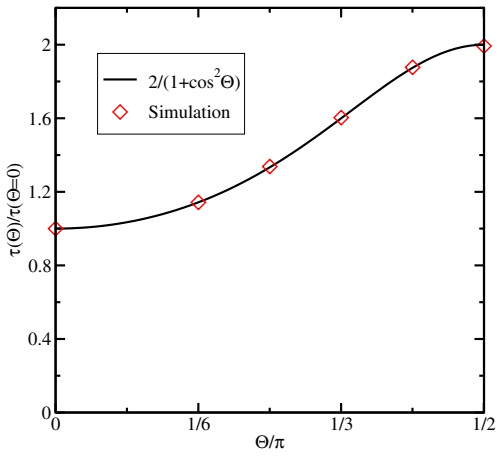

Fig. 8: Variation of τ with the valley splitting, when Θ is used as a parameter. Line: theory.

be deduced by averaging M_{SR}^2 over the in-plane momentum vector, and can be expressed as:

$$\frac{1}{\tau(\Theta)} \propto 1 + \cos^2\Theta\,, \tag{14}$$

and thus $\tau(\Theta = \frac{\pi}{2}) = 2 \cdot \tau(\Theta = 0)$. The simulated results and the analytical expression show perfect agreement. We point out that a similar ratio of spin lifetime on the injection orientation with respect to the valley orientation axis has also been reported for bulk silicon [14] [15], indicating that the result (14) is more general as it is applied in both bulk silicon and thin silicon films.

IV. Conclusion

We have discussed how shear strain-induced subband splitting causes a giant increase of spin lifetime in an SOI silicon film. We observe that this is a consequence of the reduction of the intersubband spin relaxation. We have shown that an alteration of the spin injection direction further influences the spin relaxation rates and henceforth the spin lifetime. An effective $\mathbf{k}\cdot\mathbf{p}$ Hamiltonian with the spin degree of freedom is used to find the subband wave functions and the subband energies in the presence of stress and spin-orbit interaction. As expected, the spin injection orientation does not affect the momentum relaxation time, whereas the inter- and intrasubband components of the spin lifetime are equivalently sensitive to it. This causes the total spin scattering rate (lifetime) to decrease (increase), when spin is injected along in-plane. For an in-plane injection a two-fold increment for in-plane injection is found, as compared to when the spin is injected in perpendicular-plane direction.

Acknowledgment

This work is supported by the European Research Council through the grant #247056 MOSILSPIN.

References

[1] D. E. Nikonov and I. A. Young. Overview of Beyond-CMOS Devices and a Uniform Methodology for their Benchmarking. *Proceedings of the IEEE*, 101(12):1–36, 2013.

[2] B. Huang, D. J. Monsma, and I. Appelbaum. Coherent Spin Transport through a 350 Micron Thick Silicon Wafer. *Phys. Rev. Lett.*, 99:177209, 2007.

[3] J. Li and I. Appelbaum. Modeling Spin Transport in Electrostatically-Gated Lateral-Channel Silicon Devices: Role of Interfacial Spin Relaxation. *Phys. Rev. B*, 84:165318, 2011.

[4] D. Osintsev, V. Sverdlov, N. Neophytou, and S. Selberherr. Valley Splitting and Spin Lifetime Enhancement in Strained Thin Silicon Films. *Computational Electronics (IWCE), 2014 International Workshop on*, pages 1–4, 2014.

[5] J. Ghosh, D. Osintsev, V. Sverdlov, and S. Selberherr. Dependence of Spin Lifetime on Spin Injection Orientation in Strained Silicon Films. *Ultimate Integration on Silicon (EUROSOI-ULIS), 2015 Joint International EUROSOI Workshop and International Conference on*, pages 285–288, 2015.

[6] V. Sverdlov. Strain-Induced Effects in Advanced MOSFETs. Springer, Wien-New York, 2011.

[7] P. Li and H. Dery. Spin-orbit Symmetries of Conduction Electrons in Silicon. *Phys. Rev. Lett.*, 107:107203, 2011.

[8] D. Osintsev, V. Sverdlov, and S. Selberherr. Reduction of the Surface Roughness Induced Spin Relaxation in SOI Structures: An Analytical Approach. *Conference Proceedings of the Ninth Workshop of the Thematic Network on Silicon on Insulator Technology, Devices and Circuits*, 46, 2013.

[9] M. V. Fischetti, Z. Ren, P. M. Solomon, M. Yang, and K. Rim. Six-band $\mathbf{k}\cdot\mathbf{p}$ Calculation of the Hole Mobility in Silicon Inversion Layers: Dependence on Surface Orientation, Strain, and Silicon Thickness. *J. Appl. Phys.*, 94(2):1079–1095, 2003.

[10] D. Osintsev, V. Sverdlov, T. Windbacher, and S. Selberherr. Increasing Mobility and Spin Lifetime with Shear Strain in Thin Silicon Films. *Simulation of Semiconductor Processes and Devices (SISPAD), 2014 International Conference on*, pages 193–196, 2014.

[11] Y. Song and H. Dery. Analysis of Phonon-induced Spin Relaxation Processes in Silicon. *Phys. Rev. B*, 86:085201, 2012.

[12] J. Ghosh, D. Osintsev, V. Sverdlov, and S. Selberherr. Intersubband Spin Relaxation Reduction and Spin Lifetime Enhancement by Strain in SOI Structures. *Microelectronic Engineering*, 147(0):89–91, 2015.

[13] V. Sverdlov and S. Selberherr. Silicon Spintronics: Progress and Challenges. *Physics Reports*, 585:1–40, 2015.

[14] H. Dery, Y. Song, P. Li, and I. Zutic. Silicon Spin Communication. *Appl. Phys. Lett.*, 99(8), 2011.

[15] J. L. Cheng, M. W. Wu, and J. Fabian. Theory of the Spin Relaxation of Conduction Electrons in Silicon. *Phys. Rev. Lett.*, 104:016601, 2010.